Electronic Supplementary Material (ESI) for Nanoscale.

Electronic Supplementary Information

Understanding the Atomic-level Process of CO-adsorption-driven Surface Segregation of Pd in $(AuPd)_{147}$ Bimetallic Nanoparticles

Hyesung An[†], Hyunwoo Ha[†], Mi Yoo, and Hyun You Kim[*]

Department of Materials Science and Engineering, Chungnam National University,
99 Daehak-ro, Yuseong-gu, Daejeon 34134, Republic of Korea

[†] These authors have equally contributed to this work

Corresponding Author: Prof. Hyun You Kim

Email: kimhy@cnu.ac.kr

Micro kinetic model for Pd-Au swapping

The modified micro-kinetic model[1] for initial CO-adsorption induced Pd-Au swapping occurs at the vertex site of NPs, the results of which are presented in Fig. 4a~b is as follows:

CO(g) + Au-vertex* ↔ 1CO-(Au-vertex*) (R1: 1st CO adsorption)

CO(g) + 1CO-(Au-vertex*) ↔ 2COs-(Au-vertex*) (R2: 2nd CO adsorption)

CO(g) + 2COs-(Au-vertex*) ↔ 3COs-(Au-vertex*) (R3: 3rd CO adsorption)

CO(g) + 3COs-(Au-vertex*) ↔ 4COs-(Au-vertex*) (R4: 4th CO adsorption)

4COs-(Au-vertex*) ↔ 4COs-(Pd-vertex*) (R5: 1st Pd-Au swapping, Fig. 4a)

4COs-(Pd-vertex*) ↔ 4COs-(2Pds-vertex*) (R6: 2nd Pd-Au swapping, Fig. 4b)

Because the R1~R4 are in equilibrium, their rate can be written as:

$$rate(R1) = k_1^+ p(CO)\theta_{Au-vertex}^{*} - k_1^- \theta_{Au-vertex}^{CO} = 0$$

$$\theta_{Au-vertex}^{CO} = \left({k_1^+}\big/{k_1^-} \right) p(CO)\theta_{Au-vertex}^{*} = K_1 p(CO)\theta_{Au-vertex}^{*}$$

$$rate(R2) = k_2^+ p(CO)\theta_{Au-vertex}^{CO} - k_2^- \theta_{Au-vertex}^{2CO} = 0$$

$$\theta_{Au-vertex}^{2CO} = \left({k_2^+}\big/{k_2^-} \right) p(CO)\theta_{Au-vertex}^{CO} = K_1 K_2 p(CO)^2 \theta_{Au-vertex}^{*}$$

$$rate(R3) = k_3^+ p(CO)\theta_{Au-vertex}^{2CO} - k_3^- \theta_{Au-vertex}^{3CO} = 0$$

$$\theta_{Au-vertex}^{3CO} = K_1 K_2 K_3 p(CO)^3 \theta_{Au-vertex}^{*}$$

$$rate(R4) = k_4^+ p(CO)\theta_{Au-vertex}^{3CO} - k_4^- \theta_{Au-vertex}^{4CO}$$

$$\therefore \theta_{Au-vertex}^{4CO} = K_1 K_2 K_3 K_4 p(CO)^4 \theta_{Au-vertex}^{*}$$

where K_i is the equilibrium constant for Ri, p(CO) represents the partial pressures of CO. k_i^+ and k_i^- is the forward and the backward rate constant for Ri, respectively. A binding site at the vertex (Au-vertex*) is composed of four adjacent Au-Au sites (See Fig. 2f for geometry). In order to activate the Pd-Au swapping, sequential adsorption of 4 CO molecules of which the process is described in R1~R4, is required. $\theta_{Au-vertex}^{*}$ and $\theta_{Au-vertex}^{nCO}$ represents a concentration of free adsorption sites at the vertex of NPs and that of the *n*CO-adsorbed vertex sites, respectively. The first Pd-Au swapping, R5, occurs in the presence of 4 CO molecules bound to the vertex site of NPs, 4COs-(Au-vertex*).

The equilibrium constants K_i is,

$$K_i = exp\left(\frac{-\Delta G_i}{kT}\right) = exp\left(\frac{-(\Delta E_i - T\Delta S_i + \Delta ZPE)}{kT}\right)$$

$\Delta E_i : Binding\ energy\ of\ CO\ molecule\ (see\ Fig. 2f)$

$\Delta S_1 : Entropy\ change\ involved\ in\ CO\ adsorption$

$\Delta ZPE : Zero\ point\ energy\ change\ upon\ CO\ adsorption = -0.07\ eV$

Temperature dependent standard entropy of CO was adopted from NIST webbook (http://webbook.nist.gov).

The R5 and R6 represents the 1st and the 2nd Pd-Au swapping process at vertex sites of NPs (See Fig. 4a and 4b), respectively. The rate of each reaction can be written as:

$$rate(R5) = k_5^+ \theta_{Au-vertex}^{4CO} - k_5^- \theta_{Pd-vertex}^{4CO}$$

$$rate(R6) = k_6^+ \theta_{Pd-vertex}^{4CO} - k_6^- \theta_{2Pd-vertex}^{4CO}$$

$$k_i^{+or-} = \frac{kT}{h} exp\left(\frac{-\Delta G_i^{+or-}}{kT}\right) = \frac{kT}{h} exp\left(\frac{-\left(E_{act,i}^{+or-} - T\Delta S_i^{+or-}\right)}{kT}\right)$$

$$E_{act,i}^{+or-} : Forward\ (+) or\ backward\ (-) activation\ energy\ for\ reaction\ i$$

$$\Delta S_i^{+or-} = 0$$

Applying the "steady-state" approximation, the concentration of the 1st swapped Pd, $\theta_{Pd-vertex}^{CO}$, is:

$$\frac{d\theta_{Pd-vertex}^{4CO}}{dt} = k_5^+ \theta_{Au-vertex}^{4CO} - k_6^+ \theta_{Pd-vertex}^{4CO} = 0$$

$$\theta_{Pd-vertex}^{4CO} = \frac{k_5^+}{k_6^+} \theta_{Au-vertex}^{4CO}$$

And for the 2nd swapping process of Pd,

$$\frac{d\theta_{2Pd-vertex}^{4CO}}{dt} = k_6^+ \theta_{Pd-vertex}^{4CO} - k_6^- \theta_{2Pd-vertex}^{4CO} = 0$$

$$\theta_{2Pd-vertex}^{4CO} = \frac{k_6^+}{k_6^-} \theta_{Pd-vertex}^{4CO}$$

The sum of the coverage of $\theta^{nCO}_{Au-vertex}$, $\theta^{4CO}_{Pd-vertex}$, $\theta^{4CO}_{2Pd-vertex}$, and free adsorption sites ($\theta^{*}_{Au-vertex}$) is equal to 1, so that:

$$\theta^{*}_{Au-vertex} + \theta^{1CO}_{Au-vertex} + \theta^{2CO}_{Au-vertex} + \theta^{3CO}_{Au-vertex} + \theta^{4CO}_{Au-vertex} + \theta^{4CO}_{Pd-vertex} + \theta^{4CO}_{2Pd-vertex} = 1.$$

$$\rightarrow\ \theta^{*}_{Au-vertex} + K_1 p(CO)\theta^{*}_{Au-vertex} + K_1K_2 p(CO)^2\theta^{*}_{Au-vertex} + K_1K_2K_3 p(CO)^3\theta^{*}_{Au-vertex} + K_1K_2K_3K_4 p(CO)^4\theta^{*}_{Au-vertex} + \frac{k_5^+}{k_6^+}K_1K_2K_3K_4 p(CO)^4\theta^{*}_{Au-vertex} + \frac{k_6^+}{k_6^-}\theta^{4CO}_{Pd-vertex} = 1$$

$$\therefore\ \theta^{*}_{Au-vertex} = \frac{1}{\left\{1 + K_1 p(CO)\ +\ K_1K_2 p(CO)^2 +\ K_1K_2K_3 p(CO)^3 + K_1K_2K_3K_4 p(CO)^4 + \frac{k_5^+}{k_6^+}K_1K_2K_3K_4 p(CO)^4 + \frac{k_5^+}{k_6^-}K_1K_2K_3K_4 p(CO)^4\right\}}$$

The total rate of the initial 1st and 2nd Pd-Au swapping presented in Fig. 4a and 4b, respectively, is,

$$rate^{total} = min\{rate(R5), rate(R6)\}.$$

Here, upon the 2nd Pd-Au swapping, an internal vacancy is naturally formed. Therefore, the total equilibrium number of the vacancy, is equal to $N_v \cdot \theta^{4CO}_{2Pd-vertex}$, where N_v is the number of vertex sites of NPs.

Once the R6 is preceded, an internal vacancy is formed and it penetrates into the NP and activates further Pd-Au swapping processes in the facets of NPs. The rate of vacancy diffusion is, therefore,

$$rate(vacancy\ diffusion) = \frac{kT}{h} exp\left(\frac{-\Delta G_{vac}^{+}}{kT}\right) = \frac{kT}{h} exp\left(\frac{-(E_{act}^{+} - T\Delta S_{vac}^{+})}{kT}\right)$$

E_{act}^{+} : $Activation\ energy\ for\ vacancy\ diffusion, 0.21\ eV$

$\Delta S_{vac}^{+} = 0$

The calculated rate of vacancy diffusion is order of 10^9/sec·site between 250 K to 400 K.

Under CO oxidation condition, to secure at least one internal vacancy that activates further swapping processes,

$$N_v \cdot \theta_{2Pd-vertex}^{4CO} = 1$$

$$\therefore \theta_{2Pd-vertex}^{4CO} = \frac{1}{N_v}$$

N_v is 12 for unsupported cubo-octahedral NPs, and 8 or 4 for supported NPs (see Fig. 6b).

The minimum equilibrium $\theta_{2Pd-vertex}^{4CO}$ for facile Pd-Au swapping overall NP surface is therefore, 8.33×10^{-2}, 1.25×10^{-1}, and 2.50×10^{-1}, for each case.

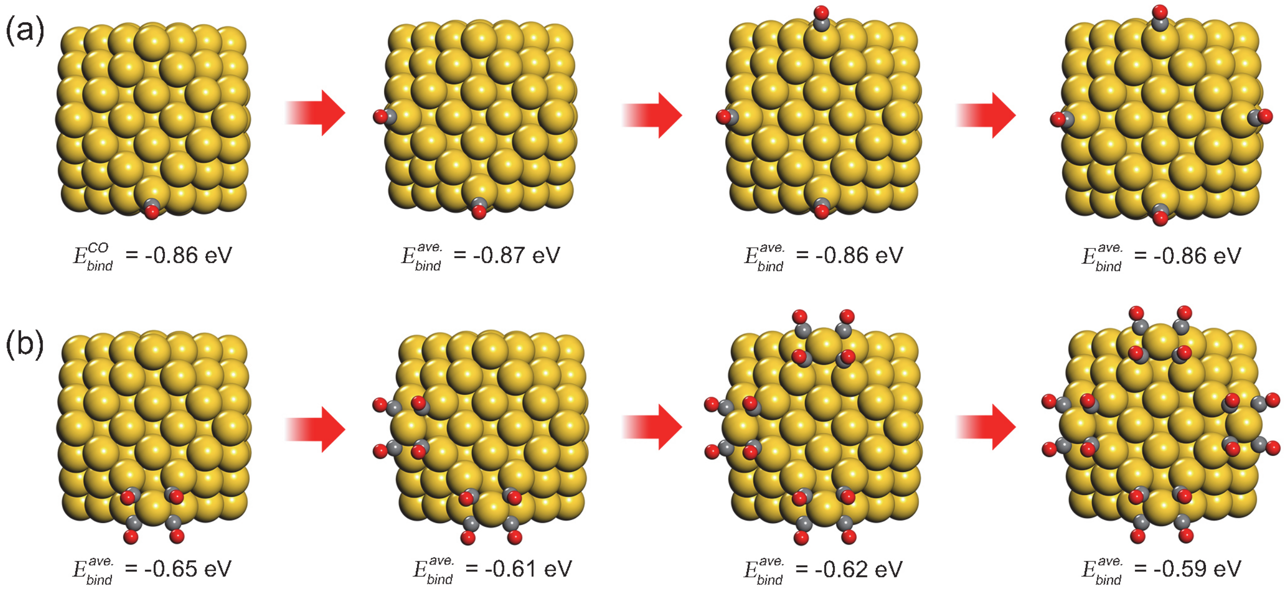

Fig. S1. The E_{bind} of CO molecules at the vertex sites of Au_{147} NP: (a) single-CO binding per single-vertex site; (b) 4 COs binding per single-vertex site. Irrespective of the number of saturated vertex sites, the E_{bind} of CO molecule(s) at the first binding vertex site does not significantly change.

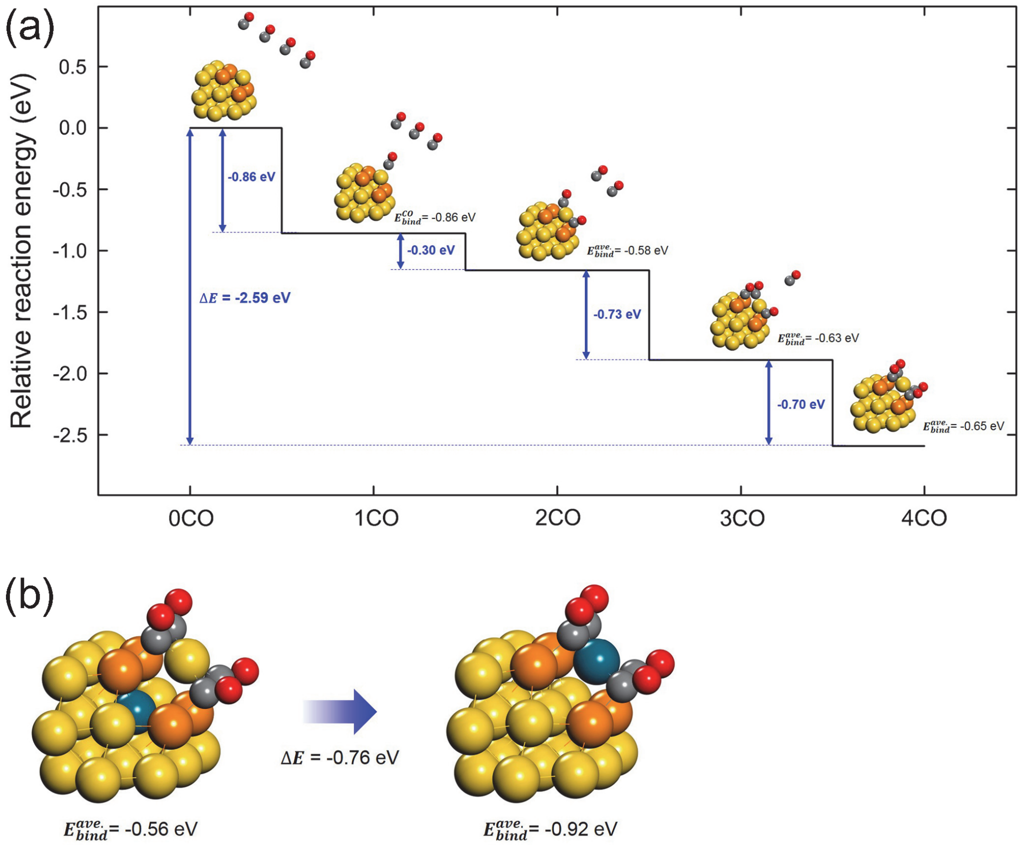

Fig. S2. Calculation scheme of E_{bind} and E. (a) E_{bind} of the n^{th}-binding CO molecule was calculated with respect to the most stable structure of NPs with n-1 CO molecules. The average E_{bind} of n CO molecules was calculated by $E^{ave}_{bind}(nCO\ molecules) = \sum E_{bind}(n^{th}\ CO\ molecules)/_{n}$. (b) The driving force of Pd segregation was simply calculated by comparing two NPs with different locations of the Pd atom.

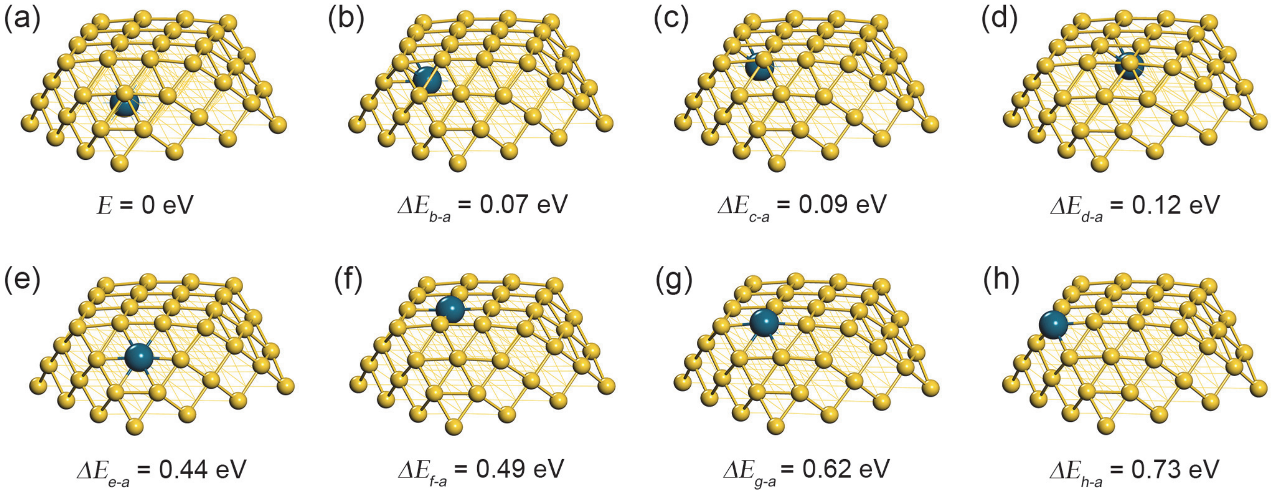

E = 0 eV

$\Delta E_{b\text{-}a}$ = 0.07 eV

$\Delta E_{c\text{-}a}$ = 0.09 eV

$\Delta E_{d\text{-}a}$ = 0.12 eV

$\Delta E_{e\text{-}a}$ = 0.44 eV

$\Delta E_{f\text{-}a}$ = 0.49 eV

$\Delta E_{g\text{-}a}$ = 0.62 eV

$\Delta E_{h\text{-}a}$ = 0.73 eV

Fig. S3. Preferred location of a Pd atom in a AuPd NP. (a) The most stable locations of a Pd atom in the Au host NP. Relative energy values corresponding to the Pd location are presented in (b)-(h). $\Delta E_{\text{x-a}}$ denotes the difference in the total energy of (x) and (a). For example, a $\Delta E_{\text{h-a}}$ of 0.73 eV means that the total energy of the NP with Pd at the vertex site (h), is 0.73 eV higher than that of the NP with Pd at the third layer from the surface (a).

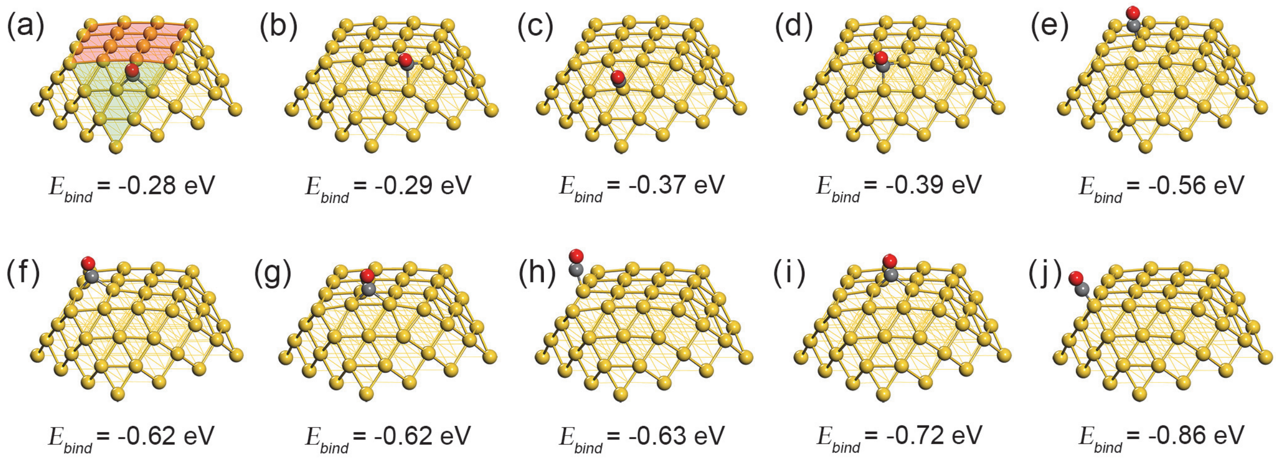

Fig. S4. Energetics and geometry of CO binding on a Au NP.

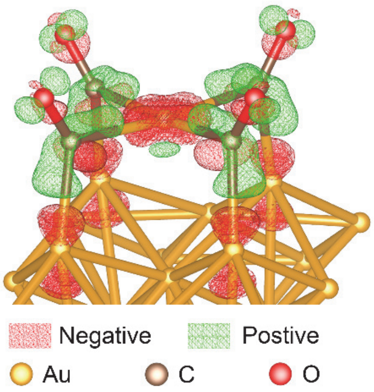

Fig. S5. Electron redistribution map upon multiple CO adsorption on the vertex site of the Au NP. The areas highlighted in red or green indicate where the electron density is accumulated or depleted.

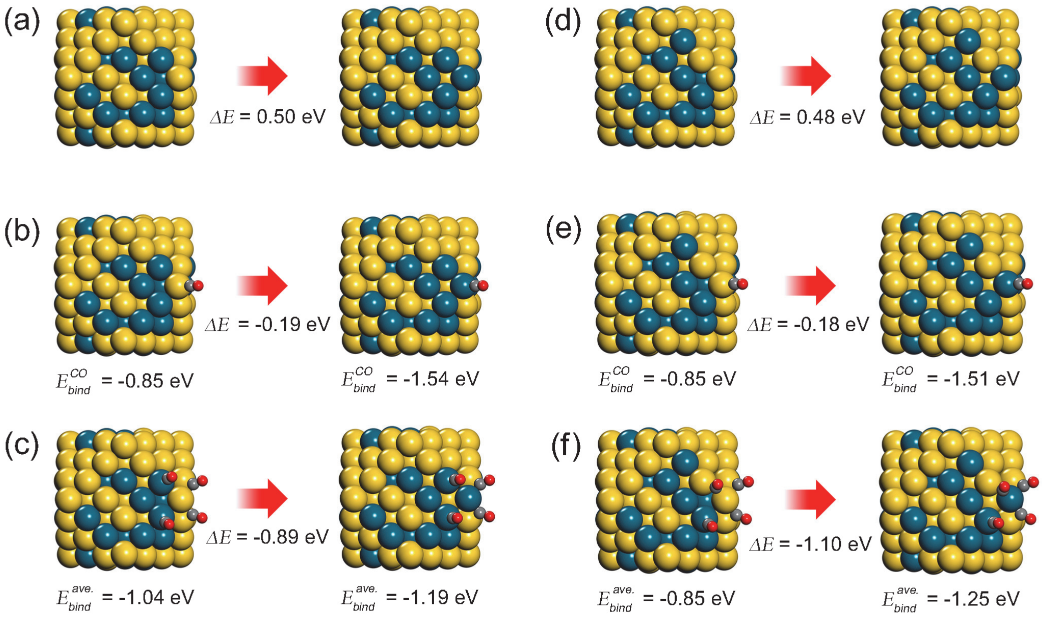

Fig. S6. Driving force of Pd-Au swapping in Au-Pd random-alloy nanoparticles. (a, d) ΔE of Pd surface segregation calculated without CO. (b, e) ΔE calculated with single pre-adsorbed CO. (c, f) ΔE calculated with four pre-adsorbed CO molecules. ΔE values calculated in (c) and (f) are not significantly different from the ΔE values presented in Fig. 3.

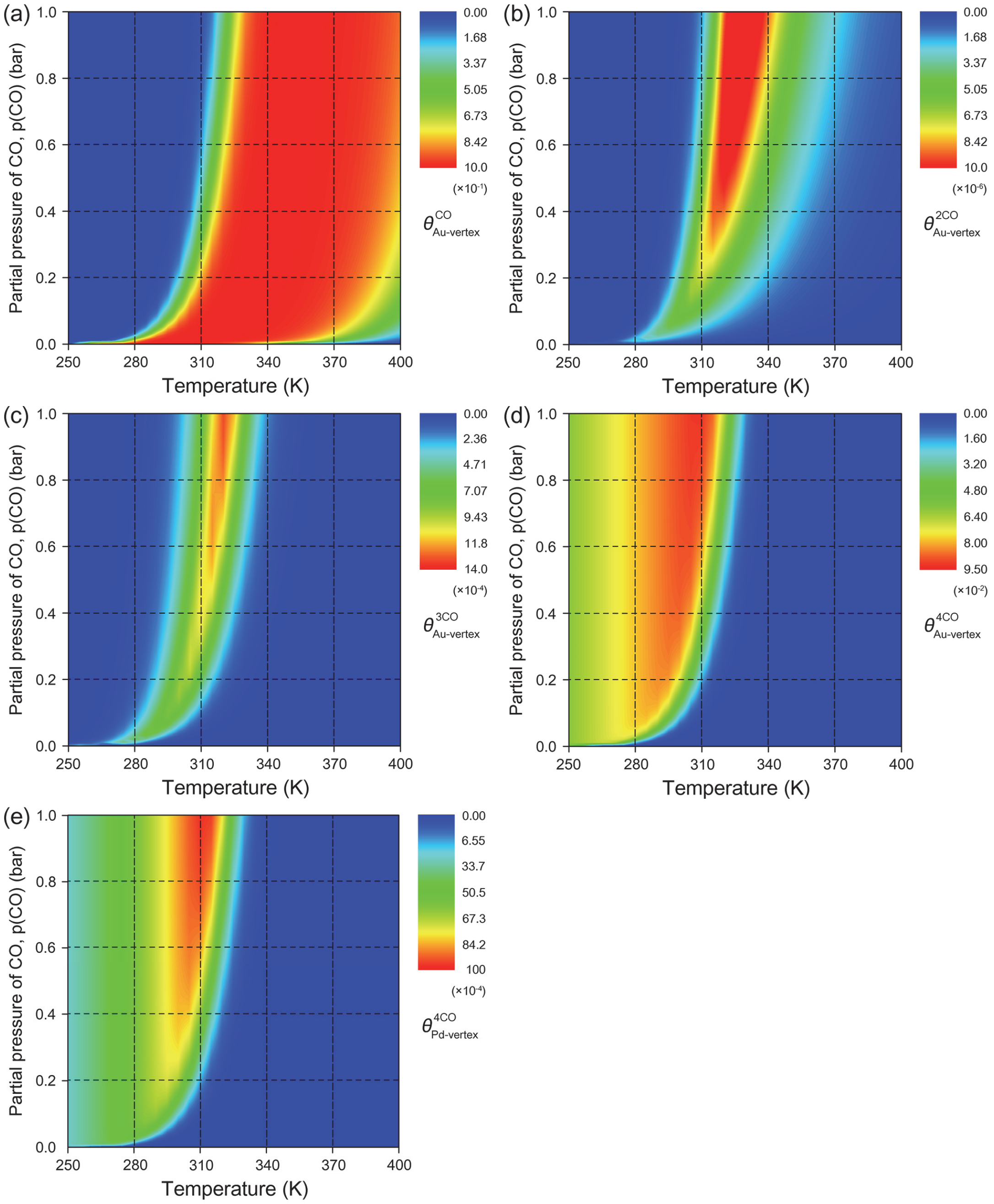

Fig. S7. Temperature-*p*(CO) maps of the equilibrium concentration of binding species on the vertex sites of a AuPd NP. (a) $\theta^{CO}_{Au-vertex}$, (b) $\theta^{2CO}_{Au-vertex}$, (c) $\theta^{3CO}_{Au-vertex}$, (d) $\theta^{4CO}_{Au-vertex}$, and (e) $\theta^{4CO}_{Pd-vertex}$.

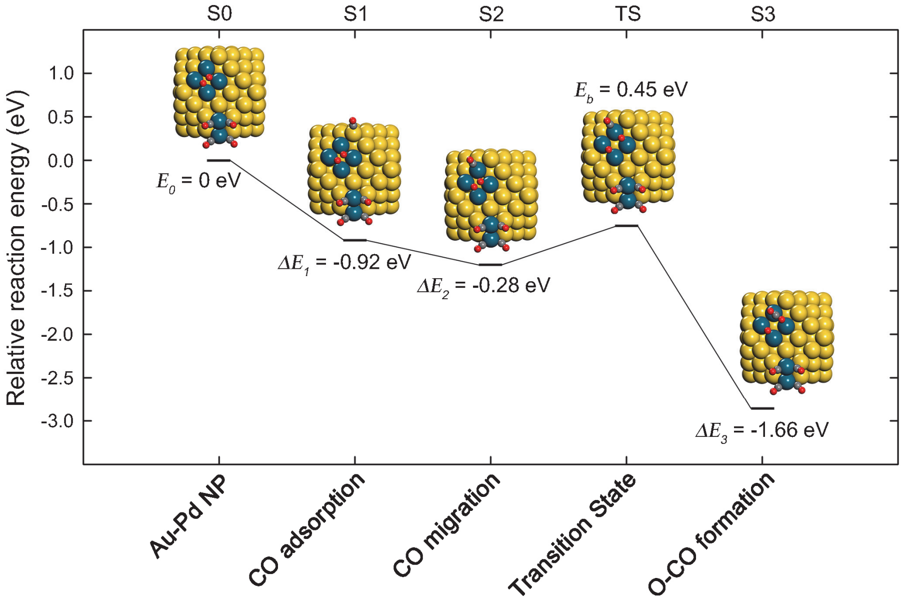

Fig. S8. Energetics of the first CO oxidation pathway at the Au-Pd interface. The dissociated oxygen atoms actively oxidize the Au-CO* at the Au-Pd interface.

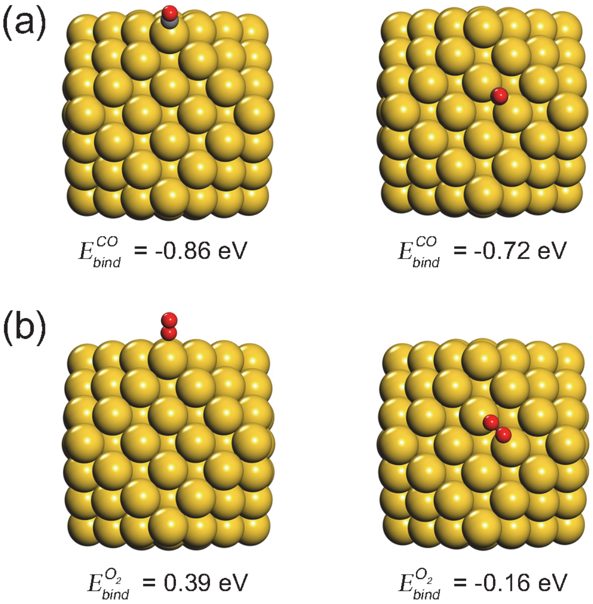

Fig. S9. The E_{bind} values of CO and O_2 on the vertex and Au(100) of a Au_{147} NP. (a) CO adsorption. (b) O_2 adsorption.

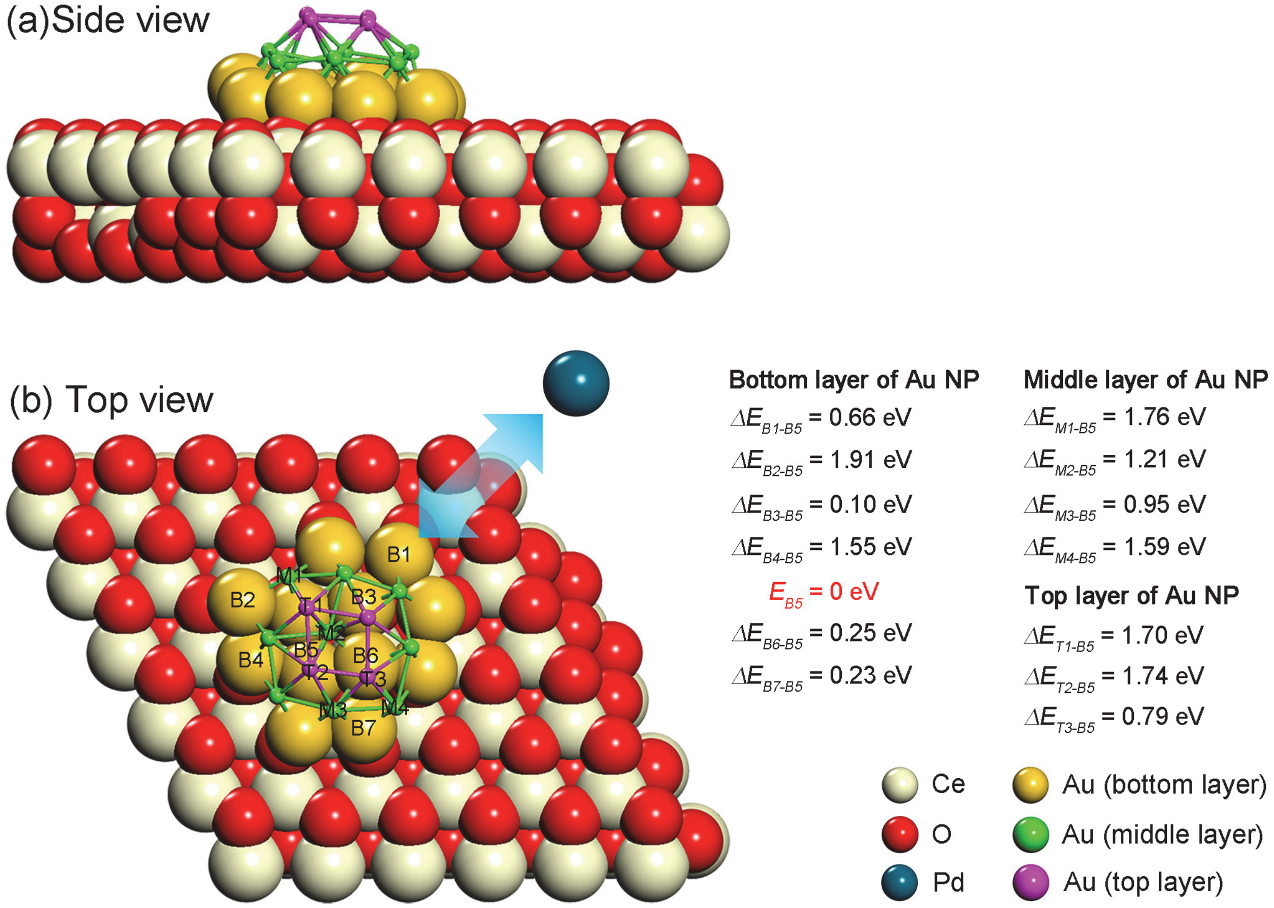

Fig. S10. Preferred location of the Pd solute atom in the $CeO_2(111)$ supported AuPd bimetallic NP.